

Separation of Polymers by Molecular Topology Using Monolithic Columns

David M. Meunier* and Patrick B. Smith

The Dow Chemical Company, Analytical Sciences Laboratory, 1897 Building,
Midland, Michigan 48667

Scott A. Baker

Rhodia Incorporated, 2151 King Street Extension, Charleston, South Carolina 29405

Received October 15, 2004; Revised Manuscript Received February 21, 2005

ABSTRACT: Long chain branching (LCB) is most often incorporated into polymeric materials to enhance rheology and processing. Presently, the characterization of LCB in polymers is limited to the determination of the number of long chain branches per molecule. The ability to characterize other branching parameters such as the molecular weight of the branch and the shape of the branched molecule (star, comb, “T”, “H”, etc.) would have considerable value in material design. A new fractionation method, molecular topology fractionation (MTF), is described herein for the separation of polymer molecules based on LCB topology. This first successful practice of MTF uses monolithic columns to create a tortuous path having macropores or flow-through channels of the order of polymer molecular dimensions as the separation medium. Because long chain branched molecules are retained more than linear molecules of the same size, the method can be used to separate branched from linear chains. Performed in a thermodynamically good solvent, the key parameters influencing the onset of MTF include flow rate, macropore dimensions, and molecular weight of the polymer to be separated. The onset of the MTF mechanism is characterized by a flow rate-dependent reversal in the elution order of narrow molecular weight polystyrene standards, denoting a distinct change in retention mechanism. Below the reversal point, retention consistent with a hydrodynamic chromatography mechanism is active. Above the reversal point, a new mechanism yields increased retention with increasing molecular weight.

Introduction

Long chain branching (LCB) in polymeric systems can be a valuable attribute because it can have significant impact on the rheological behavior of a material provided the branch lengths are significantly larger than the entanglement molecular weight.¹ Because long chain branched molecules entangle more effectively than their linear counterparts, polymers containing LCB possess considerably higher zero-shear viscosity than linear molecules of the same molecular weight. Polymers containing LCB have smaller radii of gyration than linear polymers of the same molecular weight, so they shear thin to a greater extent. This rheological behavior provides branched molecules superior processability relative to linear molecules of the same molecular weight. The elevated zero-shear viscosity due to enhanced entanglements gives additional strength to the extrudate and is often referred to as “melt strength”. Long chain branched polymer systems are often used in the production of polymer films and fibers because melt strength is important. In addition to the number of long chain branches per molecule, the molecular weight of the branch and the shape of the branch (T, star, H, comb, etc.) are also important variables. If such structural information regarding branching topology could be determined, it could be correlated with the rheological properties of the material giving rise to new structure-processing relationships for long chain branched polymers. These new relationships would undoubtedly facilitate the design of new materials to meet specific rheology targets in the market place.

The current approaches for measuring LCB in polymers are limited to the determination of the number of long chain branches per molecule. The two techniques most often used for this measurement are nuclear magnetic resonance (NMR) and size exclusion chromatography (SEC) (also called gel permeation chromatography (GPC)) together with differential viscometry (DV) and/or light scattering (LS) detectors. NMR is used to count the number of branch points per molecule.² GPC techniques compare the hydrodynamic size reduction of a branched molecule relative to a linear molecule of the same molecular weight, and with an appropriate model,³ a branch frequency corresponding to that size reduction is calculated.⁴

The separation of polymer molecules based on the number of long chain branches, the size of the branches, and the functionality of the branch site (all of these variables comprise topology) could possibly be accomplished in the following way. Because they entangle much more effectively and possess longer relaxation times, LCB polymers exhibit very different behavior in viscous media relative to linear molecules of the same molecular weight. The concentration and topology of the long chain branches both have significant influence on entanglement. Therefore, if the separation were to be conducted in a medium that would promote entanglement, the branched molecules would move through the medium more slowly than their linear counterparts. This mobility would probably also be a function of branch topology.

There are several possible ways to conduct separations in a medium in which entanglements would dominate the separation. Recently, a “microdevice” for

* Corresponding author. E-mail dmeunier@dow.com.

separating biomolecules was reported⁵ in which an array of posts, 1.5 by 6 μm in dimension, was used to create a maze of molecular dimensions through which strands of DNA were separated under the influence of a flow field. Such a device should work even more effectively for branched molecules because the branch sites would provide additional points of entanglement for the chains on the posts. However, the reported maze dimensions in the microdevice were too large to separate synthetic polymers. A device about an order of magnitude smaller (posts on the order of 0.1 μm dimensions) would be required.

Another attempt to separate macromolecules by an entanglement mechanism involved electrophoresis where a relatively high viscosity gel was used as the entanglement medium.⁶ Three separations regimes were identified for linear sulfonated polystyrene, and these regimes depended on molecular weight. Low molecular weight chains were separated by a size exclusion mechanism, while intermediate molecular weight chains were weakly entangled, and high molecular weight chains were strongly entangled in the gel. Branched sulfonated polystyrene was observed to elute by a size exclusion mechanism and not by entanglement. However, the molecular weight of these branched materials was well below that needed for effective entanglement. An electrophoresis-based separation would only be useful for a small fraction of synthetic polymers because it must be performed in a conductive medium and the polymer must have (or be derivitized to have) a charge.

A potential third approach for separating branched polymers from linear polymers involves the use of nanopores as a separation medium. Theoretical discussions of the use of nanopores for separating star polymers⁷ and statistically branched polymers⁸ have been presented. Although no experimental data were presented, it was suggested that judicious choice of nanopore diameter might allow for determination of both the molecular weight and the distance between branch points.

A fourth approach, and the one reported here, utilizes a column with a tortuous path on the order of molecular dimensions. Newly introduced column technology, referred to as monolithic columns, can be manufactured to meet this requirement.^{9–16} Monolithic columns consist of a continuous rod of porous material (most often polymer or silica based) with a bimodal pore structure termed macropores and mesopores. The lack of interparticle voids improves convective transport because all of the mobile phase is forced to flow through the column packing rather than around it. Monolithic columns typically have higher porosity compared to packed columns resulting in much lower column backpressure. The high porosity of conventional monolithic columns results from the presence of large interconnected throughpores or macropores (1–2 μm) that transport mobile phase. The surface area required for chromatographic adsorption and desorption is obtained with mesopores (10–50 nm) in the monolith. The high level of interconnectivity in the column pore structure and lack of interparticle effects produces columns with much improved performance in the higher flow rate regime. Monolithic columns have been used for a variety of high-speed separations.^{10–13,16}

The monolithic columns used in this study were produced to our specifications by a commercial vendor

to be of much smaller macropore diameter than commercially available monoliths. Because small macropore dimensions were requested, the flow and pressure characteristics of conventional monoliths were not realized with these special columns.

It should also be stated for completeness that there is one other separation mechanism postulated for macromolecules in an environment created in this manner (a tortuous path of molecular dimensions), that of an “entropy barrier” mechanism.¹⁷ As a polymer molecule migrates through restrictions smaller than its hydrodynamic volume, it must deform, thereby sacrificing entropy. This gives rise to a retention mechanism based on size, and the mechanism is also expected to have a molecular topology dependence because a branched molecule would need to sacrifice more entropy than a linear molecule as it migrated through these restrictions. Branched and linear molecules would behave very similarly as they entered the restriction, but as the branch point of the branched molecule approached the restriction, the magnitude of conformational entropy lost by the branched molecule would be larger than the linear molecule.

A novel chromatographic approach for separating linear from branched polymer molecules is described herein. The new technique, termed molecular topology fractionation (MTF), is critically dependent on the macropore dimensions within the column and the mobile phase flow rate. Separation of linear and long chain branched polymer chains was demonstrated for polystyrene (PS). The newly developed method, when combined with complementary techniques such as GPC with molecular weight sensitive detectors, should provide new information on the molecular topology or branching architecture of the polymer.

Experimental Section

Materials. Low-polydispersity, linear PS and polybutadiene (PBD) molecular weight standards used in this study were obtained from Polymer Laboratories Incorporated (Amherst, MA). Standards were typically prepared at a concentration of 0.5 mg/mL in unstabilized tetrahydrofuran (THF), and the solutions were stored in the dark at 5 °C when not in use. All references to PS or PBD standard molecular weights are peak molecular weights (M_p), and these were provided by the vendor.

Randomly branched PS samples were obtained in-house and were prepared by coupling polystyryl dianion of a specified molecular weight using α,α' -dichloro-*p*-xylene and α,α',α'' -trichloromesitylene as the coupling reagents. The branching density in these samples depends on the mole fraction of trifunctional coupling reagent, the extent of reaction, the mole fraction of polystyrene dianion, and the molecular weight of the dianion, while the molecular weight of the final polymer depends on the molecular weight of the polystyryl dianion, the stoichiometric balance between styryl anions and coupling groups, and the extent of reaction. More details on the preparation of the branched PS samples used in this study can be found elsewhere.¹⁸

Several comb-branched PBD samples were also used in this study. Details of the synthesis and characterization of these materials can be found elsewhere.¹⁹ The nominal backbone/side chain molecular weights of the comb branched samples in kg/mol were 100/20, 100/15, 100/5, 85/20, 65/20, 50/25, 50/20, 50/15, and 50/10.

Molecular Topology Fractionation. Uninhibited THF (Fisher HPLC grade) was used as the mobile phase for all MTF experiments. Several different LC systems were used for MTF experiments. The primary system for UV detection studies consisted of a Waters 510 HPLC pump (Waters Corp., Milford,

Table 1. Flow Characteristics and Macropore Dimensions of Polystyrene/Divinylbenzene Monolithic Columns Used for MTF Studies

column no.	flow rate (mL/min) at 10 MPa pressure drop	macropore diameter (μm) measured ^a	macropore diameter (μm) calculated ^b	pore volume fraction ^f	pore volume fraction ^g
1	0.10	0.113	0.161	0.63	0.65
2	0.20		0.205	0.69	
3	0.007		0.097	0.12	
4	> 35 ^c		> 0.5 ^d	0.49	
5	0.025		0.206 ^e		
6	0.075		0.237 ^e		
7	0.26	0.192	0.270	0.58	0.62
8	1.78		0.655	0.67	

^a The pore sizes of these columns were determined by mercury porosimetry with a precision of 3% RSD. ^b These values were calculated using the Kozeny–Carman equation using the flow rate and pressure drop information in the table.²⁰ ^c This value is estimated based on a 2.7 MPa pressure drop for a 10 mL/min flow rate. ^d This value is estimated based on discussion with vendor. ^e Columns 5 and 6 exhibited very low porosity of ~10% and 20%, respectively. ^f Based on elution volume of a small molecule such as toluene. ^g Based on mercury intrusion volume.

MA) operated at flow rates from 4 to 100 $\mu\text{L}/\text{min}$, a pulse dampener, a Kratos Spectroflow 773 UV detector at 254 nm (Ramsey, NJ), an Alcott 728 autosampler (Atlanta, GA), and a Rheodyne injection valve (Rohnert Park, CA). A fixed volume injection loop of 5 μL was used. A flow splitter was necessary to achieve flow rates less than 100 $\mu\text{L}/\text{min}$ with this system. An LC Packings IC-400-VAR variable flow splitter module (San Francisco, CA) was used with a 130 cm section of 25 μm i.d. fused silica capillary (as a restrictor) to provide the proper flow rate. For example, a pump setting of 1 mL/min provided a flow rate of approximately 20 $\mu\text{L}/\text{min}$. The exact flow out of the splitting device was dependent on the total restriction from the capillary restrictor and column. Some UV detection experiments were also performed on an HP 1090 LC system (Agilent Technologies, Palo Alto, CA).

For evaporative light scattering detection (ELSD) studies, an Agilent 1100 LC system with photodiode array (PDA) detection was coupled with an Alltech 500 ELSD (Alltech, Deerfield, IL). Because the total volume of the tubing and connections from the PDA to the ELSD was only 30 μL , an insignificant amount of band broadening was introduced between detectors. Because of the very low THF flow rates used for MTF compared to normal chromatographic operation, ELSD conditions (drift tube temperature and gas flow) were optimized. At a flow rate of 10 $\mu\text{L}/\text{min}$, the optimum tube temperature and gas flow (argon) was 35 °C and 1.0 L/min, respectively.

Monolithic Columns. The columns used in this work were custom-made by ISCO Inc. (Lincoln, NE). They are poorly suited for conventional HPLC because of the high backpressure resulting from the small macropore dimensions. The macropore dimensions in two of the columns used in this study were determined by mercury porosimetry analysis, and these results can be found in Table 1. The monolithic columns were composed of poly(styrene-co-divinylbenzene). These were chosen on the basis of their availability and also because of reduced likelihood of enthalpic interactions between the polymers under study and the column material. The column dimensions were 50 mm \times 4.6 mm i.d.

Solvent Fractionation of Branched PS. Precipitation of a high molecular weight fraction from a polydisperse polymer sample containing LCB was used to obtain a relatively narrow distribution polymer fraction with LCB for MTF studies. A polymer solution (5 mg/mL in THF) was titrated with methanol to the cloud point. The suspension was then centrifuged, the supernatant was decanted, and the remaining solids were evaporated to dryness. The high molecular weight solid material was then redissolved in THF and characterized by GPC and MTF.

GPC Measurements. Gel permeation chromatography (GPC) was used extensively to provide linear PS-equivalent weight-average molecular weights (M_w) and molecular weight distributions for the samples used in this study. Measurements were carried out in THF at a flow rate of 1 mL/min using a Waters Alliance 2690 with both UV and RI detection. Column sets consisted of either three mixed-B or mixed-C columns

(Polymer Laboratories, Amherst, MA). An injection volume of 50 μL was used (solution concentrations of 0.5–2 mg/mL). Narrow molecular weight distribution PS standards from Polymer Laboratories (Amherst, MA) were used to calibrate the GPC columns. Thus, references to molecular weight are linear PS-equivalent M_w values unless specified otherwise.

Results and Discussion

The hypothesis of this work is that polymer molecules will migrate at rates dependent on their LCB topology when forced to flow through channels having size dimensions of similar order to their molecular dimensions. The optimum stationary phase for this separation would possess channel sizes of roughly the size of the molecule to be separated, would have high pore volume to minimize backpressure and shear fields, and would be inert, providing no enthalpic interactions between the stationary phase and the polymer analyte. The following discussion evaluates the effect of these variables on the separation.

Effect of Macropore Size. Monolithic columns, whose macropore dimensions were of similar order to molecular dimensions, provided the initial medium to test our hypothesis. Indeed, extended polymer chains of sufficient size were observed to exhibit retention behavior consistent with, but not proof of, an entanglement mechanism as they were forced by flow to migrate through these specially designed monolithic columns. Such behavior was observed provided the macropore sizes were of the appropriate dimensions and there was sufficient time for interaction to occur.

A study of the retention behavior of linear PS standards on the monolithic columns provided information on the relationship between molecular size and macropore size on the separation mechanism. The log M_p vs peak elution volume plots for the various columns are shown in Figure 1. The plots were linear with a negative slope for linear PS chains that were small relative to the column macropore dimensions. Such behavior is consistent with a hydrodynamic chromatography (HDC) retention mechanism. The same elution order would also be observed if the small molecules were retained by a GPC mechanism. However, a GPC mechanism is unlikely for these columns because the columns do not appear to have any stagnant pores or mesopores in the appropriate size range for GPC. If molecules were to interact with the stationary phase of the column by entanglement and/or entropy barrier mechanisms, they would be retained longer than predicted by an HDC mechanism. As described above, LCB chains would be expected to be retained longer than linear chains of the

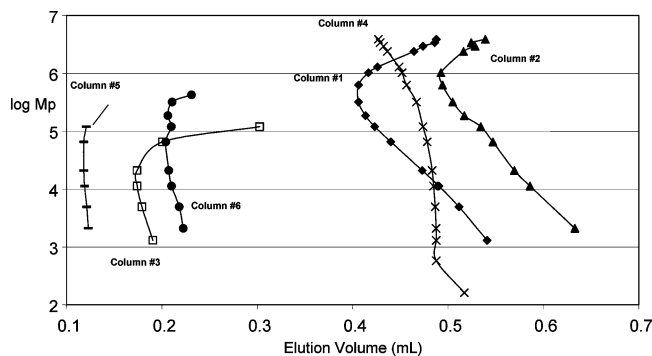


Figure 1. Log M_p vs peak elution volume for linear PS narrow molecular weight standards obtained on monolithic columns.

same molecular weight. As such, a reversal of the elution order would be observed when polymer chains, either branched or linear, interact on the column in this way. A reversal in the plot was observed when columns having the appropriate tortuous path dimensions were used.

The additional retention (beyond that predicted by HDC) of higher M_p PS standards was demonstrated by the reversal in the log M_p vs elution volume plots observed for monolithic columns 1–3. Column 4, a typical commercial monolith, did not show the reversal effect over the molecular weight range studied because this column possessed macropore dimensions too large relative to the macromolecular dimensions of the polymers studied ($\sim 1 \mu\text{m}$ macropores and 10 nm mesopores per ref 11). The fact that column 4 did not show a reversal demonstrated that the mechanism of retention in the reversal region was not due to adsorption because the columns differed only in pore size, not chemical composition. Column 3 contained the smallest macropores, and the reversal occurred at the lowest molecular weight ($\sim 15 \text{ kg/mol}$) among the columns studied. There was only a small difference in the macropore dimensions within the tortuous path in columns 1 and 2, resulting in a slightly different reversal molecular weight (~ 400 and 1000 kg/mol , respectively). Thus, the reversal point was dependent on the macropore dimensions within the column. The smaller the macropore sizes, the lower the reversal molecular weight.

The Carman–Kozeny (C–K) relationship²⁰ can be used to predict the average pore diameter from column porosity and pressure drop data. The flow rates required to yield a 10 MPa column pressure drop were determined for each of the columns (see Table 1). For a given column porosity, this flow rate value was an indicator of the average macropore size of the tortuous path within the particular monolithic column, with smaller flow rates being indicative of smaller macropore sizes. These predictions are also given in Table 1. For comparison purposes, two of the columns were characterized by mercury porosimetry, and these results also appear in Table 1. It is clear that the sizes predicted by the C–K relationship are larger than those measured by mercury porosimetry by a factor of about 1.4. However, considering the differences in experimental conditions for these two measurements, the agreement is reasonable. The size data measured by mercury porosimetry indicated that the monolithic columns exhibited a unimodal size distribution in the size range of 3 nm to $350 \mu\text{m}$, in contrast to the bimodal distribution (macropores and mesopores) observed for typical monolithic columns.

Resolution also appeared to be a function of macropore size. The slope of the log M_p vs elution volume plot in the reversal region comprises one component of resolution. The slopes of these plots appeared to become more flat as the macropore size was decreased, indicating that resolution improved with decreasing macropore dimension. The overall resolution of the separation depends not only on the slope of the log M_p vs elution volume plot but also on the bandwidth of the peaks. Figure 2 shows typical MTF fractograms for the linear PS standards having M_p values below and above the reversal point and for two different flow rates. An evaporative light scattering detector (ELSD) was used to acquire the fractograms shown in Figure 2. Because the ELSD response is flow rate dependent, one cannot use the data in Figure 2 to draw conclusions regarding solute recovery as a function of molecular weight and flow rate. However, data acquired with a UV absorbance detector indicated that quantitative recoveries were obtained for linear chains eluting from columns 1 and 2 for all flow rates and molecular weights studied. For the smaller macropore dimension columns (columns 3, 5, and 6) recoveries were poor above the reversal molecular weight.

Effect of Flow Rate. The flow rate dependence of linear PS retention is demonstrated in Figure 3. The log M_p vs elution volume curves for flow rates from 10 to $100 \mu\text{L/min}$ are provided. No reversal in retention was observed for flow rates of 60 and $100 \mu\text{L/min}$. The elution order reversal became more pronounced as the flow rate of the mobile phase decreased. The effect of flow rate on the magnitude of retention in the reversal regime indicated the importance of kinetics in the separation mechanism. For separation to occur, a polymer molecule must be provided kinetic opportunity to interact with the monolithic column. The column may be envisioned as containing a series of restrictions and intersections within the macropores. As a polymer molecule flows near a restriction or intersection, it must be provided enough time relative to its rheological relaxation time to interact with the stationary phase and thereby be retained. If the chain were flowing too fast relative to its relaxation time, this interaction would be suppressed. Also, the shear fields within the macropores are enhanced as the flow rate increases such that polymer molecules are shear aligned, diminishing a chain's opportunity to interact within the column.

The use of these low flow rates did not contribute to substantially increased band broadening in the reversal region. Theoretical plates per meter were determined for the fractograms shown in Figure 2 and are reported in Table 2.

Effect of Sample Concentration. To most effectively separate polymers by an entanglement mechanism, samples should be dissolved in a thermodynamically good solvent at low enough concentration to minimize polymer–polymer interactions. Figure 4 shows the effect of concentration on the log M_p vs elution volume plot for linear PS molecular weight standards. A constant injection volume was maintained, while the polymer concentrations were varied over the range of 0.5–5.0 mg/mL. For concentrations of 2.5 mg/mL and lower, there was little variation in the peak elution volumes of the standards. However, for concentrations of 5 mg/mL, significant changes in elution volume were observed for the higher M_p standards. For PS molecular weights greater than $\sim 900 \text{ kg/mol}$, concentrations ex-

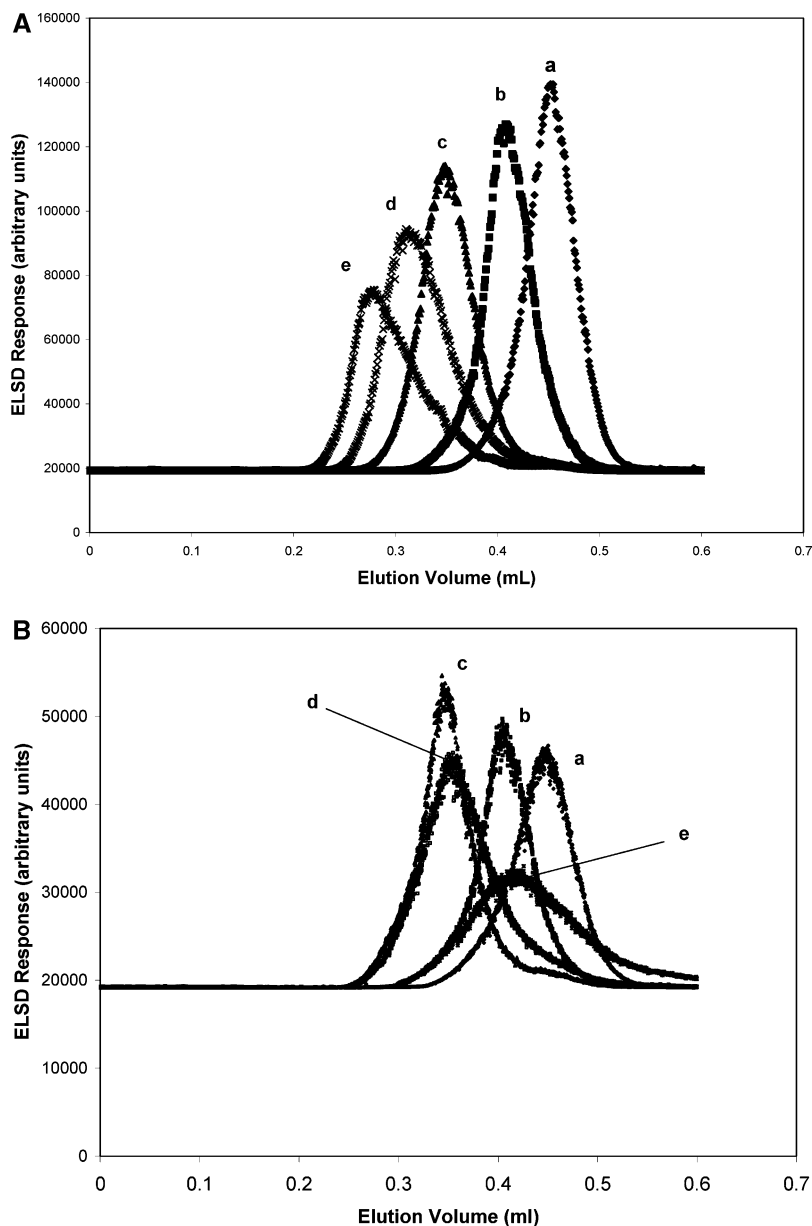


Figure 2. MTF fractograms of linear polystyrene standards of molecular weight (a) 1.30, (b) 11.3, (c) 120, (d) 1030, and (e) 3900 kg/mol obtained at a flow rate of (A) 0.050 and (B) 0.01 mL/min on column 1.

ceeding 5 mg/mL (in THF) exceed the critical concentration, C^* . These results indicated that the polymer concentration should be kept below C^* to minimize any significant concentration-related effects.

Elution Behavior of PBD. The molecular weight dependence of linear PBD elution was consistent with that observed for linear PS (Figure 5A). The reversal appeared to occur at slightly lower molecular weight compared to PS when plotted on an absolute molecular weight basis. However, when the PBD data were plotted in terms of the PS apparent M_w (from GPC data), the reversal point was essentially the same for both PS and PBD (Figure 5B). The reversal molecular weight for both PS and PBD represent degrees of polymerization of ~ 3800 and 2000 , respectively. Considering that a repeat unit of PS contains two backbone carbon atoms and a repeat unit of PBD contains four carbon atoms, the reversal points for both systems represent roughly the same number of backbone carbon atoms.

Studies with Branched PS: Fractionation of High Molecular Weight Component with Metha-

nol. Standard branched materials of narrow polydispersity and designed branch shape can be prepared,²¹ and mechanistic investigations of such materials using MTF will be the source of a future publication. However, in the absence of these standards, an existing broad molecular weight distribution, branched polystyrene sample was solvent-fractionated (see Experimental Section for details). A high molecular weight fraction was precipitated from THF solution via the addition of methanol. Figure 6A shows the linear PS equivalent molecular weight distribution for the fraction obtained from GPC. The fraction is relatively narrow in size and exhibits a linear equivalent weight-average molecular weight of 1900 kg/mol. Figure 6B shows the MTF elution profile of the fraction obtained on column 1 at a flow rate of 0.01 mL/min. The MTF elution profile of the high molecular weight fraction exhibited a bimodal fractogram. Because an evaporative light scattering detector was used, all observed modes represent nonvolatile, polymeric components. The linear equivalent M_p values corresponding to the peaks of the two modes (based on

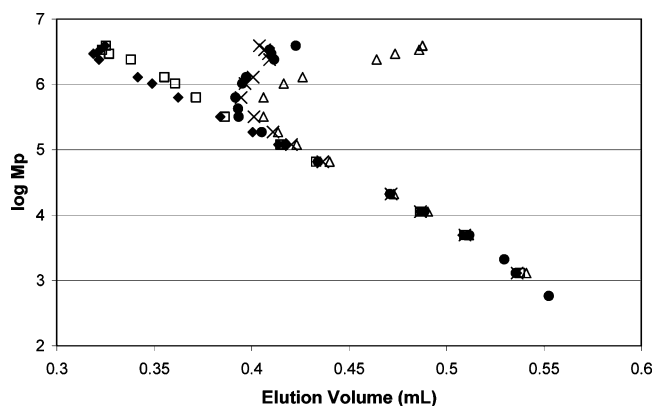


Figure 3. Flow rate dependence of $\log M_p$ vs peak elution volume for linear PS narrow molecular weight standards on monolithic column 1 as a function of flow rate: closed diamonds, 100 $\mu\text{L}/\text{min}$; open squares, 60 $\mu\text{L}/\text{min}$; x, 20 $\mu\text{L}/\text{min}$; closed circles, 15 $\mu\text{L}/\text{min}$; open triangles, 10 $\mu\text{L}/\text{min}$.

Table 2. Theoretical Plates per Meter (N/m) Calculated from the Fractograms Shown in Figure 2

mol wt (kg/mol)	plates/m (0.01 mL/min)	plates/m (0.05 mL/min)
1.30	5700	7500
11.3	6000	6100
120	3400	4400
1030	2300	1800
3900	1300	1500

linear PS standard calibration above the reversal point) were ~ 2000 and ~ 8000 kg/mol for the earlier and later eluting modes, respectively. The 2000 kg/mol mode is in excellent agreement with the molecular weight obtained by GPC and, as such, most likely corresponds to any linear chains in the fraction. The latter eluting mode may represent the branched chains in the fraction. The relative peak areas suggest that the linear component is present at a significantly higher concentration than the branched component, in contradiction to expectations, but the MTF fractogram (Figure 6B) most likely overestimates the linear chain concentration. The overestimation stems from the fact that most LCB PS samples (see section below) did not completely elute from the column, whereas quantitative recoveries were obtained for linear PS standards under these MTF conditions.

Broad molecular weight distribution PS materials containing long chain branching and of varying weight-average molecular weight, M_w , were injected onto MTF column 1 under the same flow rate conditions that yielded a reversal point for linear PS. The branched materials did not completely elute from the column within the range of practical experimental times. However, at a flow rate that yielded an HDC mechanism for linear chains, the samples containing long chain branched molecules did elute from the column. For samples having linear PS equivalent M_w values in excess of 1000 kg/mol, the peak retention volumes were larger than predicted by an HDC mechanism (Figure 7). This large flow rate dependence suggests that branched molecules must be separated in an entirely different experimental regime than linear molecules due to their much greater retention on the column.

The monolithic column macropore size dependence of this experiment is further demonstrated in Figure 8 where the same series of samples as shown in Figure 7 was analyzed with a larger macropore size monolithic

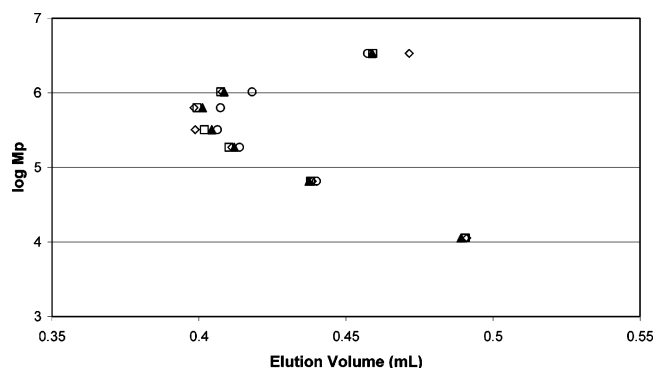


Figure 4. $\log M_p$ vs peak elution volume for varying concentrations of linear PS narrow molecular weight standards injected onto monolithic column 1 at a flow rate of 10 $\mu\text{L}/\text{min}$ and constant injection volume: open diamonds, 0.5 mg/mL; open squares, 1 mg/mL; closed triangles, 2.5 mg/mL; open circles, 5 mg/mL.

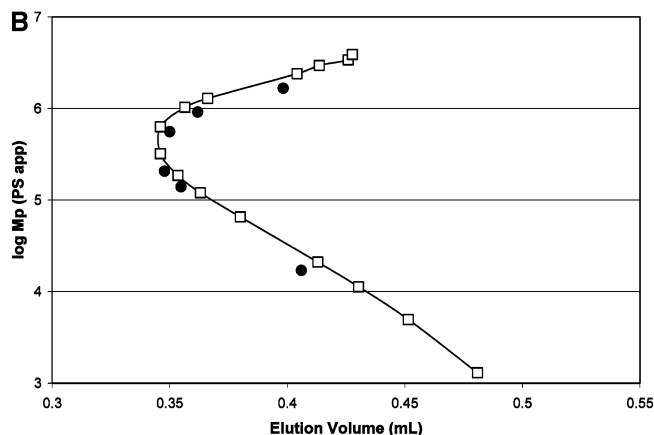
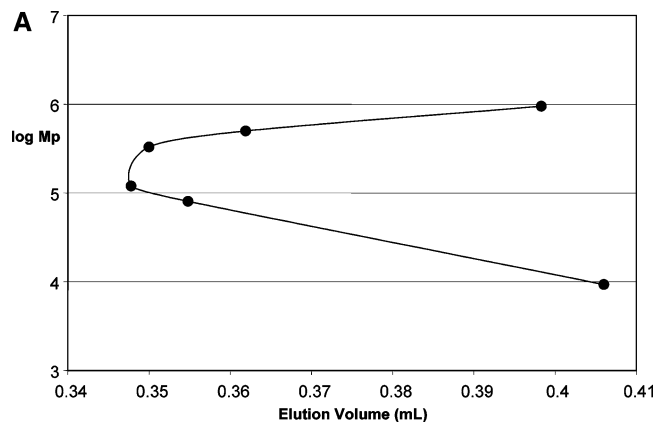


Figure 5. $\log M_p$ vs peak elution volume for linear PBD narrow molecular weight standards obtained on monolithic column 1 at a flow rate of 10 $\mu\text{L}/\text{min}$ (A) using absolute M_p values for the PBD standards to construct the plot and (B) using linear PS equivalent M_p values to construct the plot. The retention volumes for linear polystyrene standards (open squares) are given for comparison.

column denoted column 8. The elution order reversal was not observed, even at 10 $\mu\text{L}/\text{min}$ for column 8. The average macropore size predicted by the C–K relationship for column 8 was a factor of 4 larger than that of column 1 (see Table 1).

Studies with Branched Poly(butadiene). Comb-branched poly(butadiene) materials with branch lengths of roughly 5–25 kg/mol and a 3-arm star-branched PBD having 100 kg/mol arms were characterized by both GPC and MTF. Figure 9 shows the plot of $\log M_w$

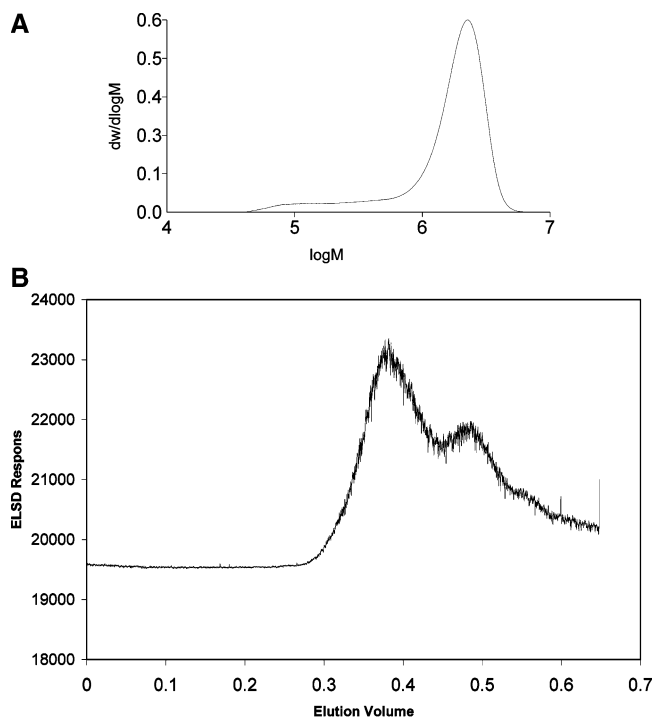


Figure 6. MTF elution volume profile and PS equivalent molecular weight distribution of a high molecular weight fraction isolated via solvent fractionation of randomly branched PS sample (A) the PS equivalent molecular weight distribution of the high molecular weight branched polymer fraction as determined by GPC and (B) the MTF elution profile of the precipitated fraction.

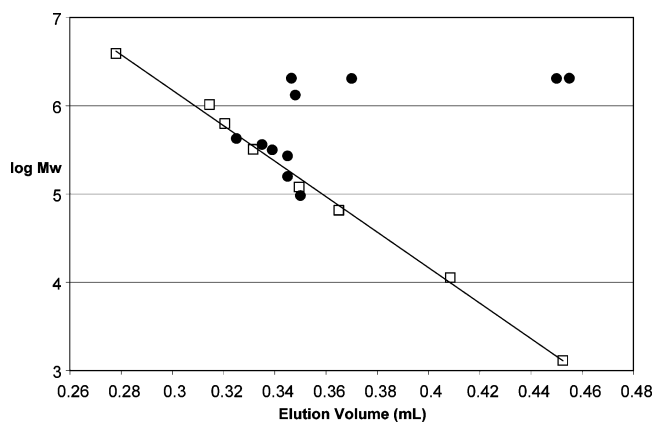


Figure 7. $\log M_w$ vs peak elution volume plot for linear (open squares) and branched PS (closed circles) obtained at a flow rate of $50 \mu\text{L}/\text{min}$ on column 1.

(PS apparent) vs elution volume for these materials and linear PS standards. No additional retention of these branched molecules relative to their linear counterparts was observed. Two conclusions can be drawn from these experiments. First, the separation mechanism in this experiment does not appear to be consistent with an entropy barrier mechanism. If it were, then the comb-branched material containing several branch points per molecule would have been retained relative to linear molecules of the same size. The second conclusion is that for an entanglement mechanism the LCBs (and also the primary chain molecular weight which was sufficient in this case for only three of the samples) must be above the reversal molecular weight for the column. The only LCB polymer in this study (3-arm star) did not exceed the reversal molecular weight of this column. A rela-

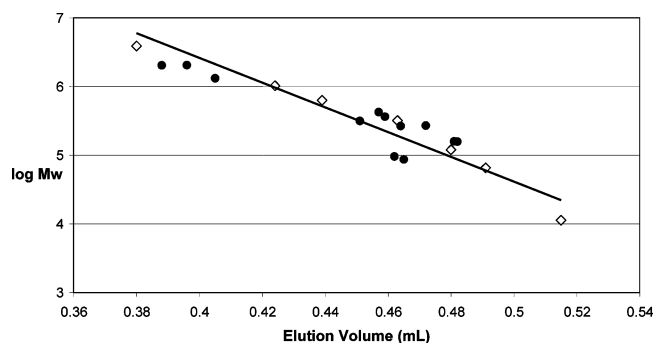


Figure 8. $\log M_w$ vs elution volume plot for linear (open squares) and branched PS (closed circles) obtained at a flow rate of $100 \mu\text{L}/\text{min}$ on column 8.

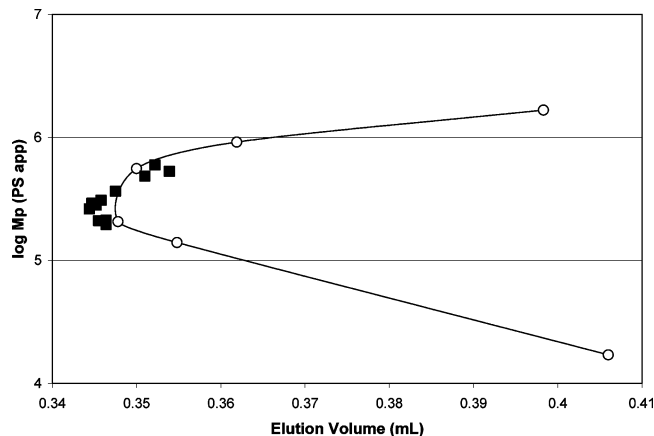


Figure 9. $\log M_p$ vs peak elution volume plot for linear (open circles) and branched (closed squares) PBD obtained at a flow rate of $50 \mu\text{L}/\text{min}$ using monolithic column 1.

tionship exists between macropore size and molecular size that must be matched in order for retention on the column to occur. Matching this relationship for the primary polymer chain may mismatch it for LCB's that are below a given molecular weight. Perhaps this technique could differentiate between linear and branched molecules, where the branch length is short, with proper choice of macropore size and flow rate.

Conclusions

A new polymer separation technique²² has been demonstrated. Although not clearly defined, the mechanism appears to be consistent with anomalous flow in confined spaces due to either entanglement or entropy barrier mechanisms. Results with PS samples indicate that the technique is capable of discriminating between linear and branched materials of the same hydrodynamic volume (i.e., components that coelute in a GPC experiment). A major challenge in separating long chain branched molecules from linear molecules is that molecular weight distributions and long chain branching distributions of synthetic polymers are typically broad. As such, separation of broad distribution LCB materials based on MTF may result in the coelution of very large long chain branched molecules with smaller, linear molecules. To optimize the separation, one could inject fractions of coeluting species from the MTF experiment onto a conventional GPC column so that the separation in the second dimension takes place via hydrodynamic volume. This 2-dimensional separation, the first dimension according to MTF and the second based on hydrodynamic size, or vice versa, should give rise to a clean

separation of linear from branched species and perhaps even separate molecules of different branching shape. Additional experiments need to be conducted with well-characterized polymers of various branching architectures and molecular weight to more clearly define what information can be gained from this technique.

In addition to examining new polymers, the separation medium needs to be more thoroughly examined. Results for high molecular weight, branched materials clearly indicated that some polymer fraction was not fully eluted from the column for all experimental conditions. If the column pore size can be accurately controlled, a systematic study of the effects of pore size on retention can be conducted. In this way, the separation medium might be designed to provide selectivity for a particular polymer molecular size range. The evaluation of alternative media (e.g., silica-based monoliths, templated polymers, or nanofabricated arrays) should also be pursued with regard to producing a medium that enhances MTF effects relative to other separation mechanisms, such as HDC and GPC. By doing so, one would increase the information content of a 2-D separation scheme based on size (by GPC or HDC) in one dimension and MTF in the other.

Finally, a thorough molecular modeling investigation of this separation mechanism is needed to clearly define the relative contributions of entanglement and entropy barrier mechanisms and to develop experimental strategies to differentiate between them as well as optimize the chromatography.

Acknowledgment. The authors acknowledge Dr. Larry Whiting of the Dow Chemical Company and Professor Robert Prud'homme of Princeton University for helpful discussions during the ideation of this work. We thank Richard Chafin of the Dow Chemical Company for mercury porosimetry analysis of the monoliths. Finally, we thank Drs. Jerry Hahnfeld and Drew Poche of the Dow Chemical Company for providing branched materials.

References and Notes

- (1) Macosko, C. W. *Rheology, Principles, Applications and Measurements*; Wiley-VCH: New York, 1994; p 505.
- (2) NMR and Macromolecules; Randall, Jr., J. C., Ed.; American Chemical Society: Washington, DC, 1984; Chapter 9.
- (3) Zimm, B. H.; Stockmayer, W. H. *J. Chem. Phys.* **1949**, *17*, 1301.
- (4) Wood-Adams, P. M.; Dealy, J. M.; deGroot, A. W.; Redwine, O. D. *Macromolecules* **2000**, *33*, 7489–7499.
- (5) Duke, T. A. J.; Austin, R. H. *Phys. Rev. Lett.* **1998**, *80*, 1552–1555.
- (6) Smisek, D. L.; Hoagland, D. A. *Science* **1990**, *248*, 1221–1223.
- (7) Brochard-Wyart, F.; de Gennes, P. G. *C. R. Acad. Sci. Paris* **1996**, *323II*, 473–479.
- (8) Gay, C.; de Gennes, P. G.; Raphael, E.; Brochard-Wyart, F. *Macromolecules* **1996**, *29*, 8379–8382.
- (9) Svec, F.; Fréchet, J. M. J. *Ind. Eng. Chem. Res.* **1999**, *38*, 34–38.
- (10) Petro, M.; Svec, F.; Fréchet, J. M. J. *J. Chromatogr. A* **1996**, *752*, 59–66.
- (11) Wang, Q. C.; Svec, F.; Fréchet, J. M. J. *Anal. Chem.* **1993**, *65*, 2243–2248.
- (12) Janco, M.; Sykora, D.; Svec, F.; Fréchet, J. M. J.; Schweer, J.; Holm, R. *J. Polym. Sci., Part A: Polym. Chem.* **2000**, *38*, 2767–2778.
- (13) Cabrera, K.; Lubda, D.; Eggenweiler, H.-M.; Minakuchi, H.; Nakanishi, K. *J. High Resolut. Chromatogr.* **2000**, *23*, 93–99.
- (14) Ishizuka, N.; Minakuchi, H.; Nakanishi, K.; Soga, N.; Tanaka, N. *J. Chromatogr. A* **1998**, *797*, 133–137.
- (15) Reigner, F. E. *J. High Resolut. Chromatogr.* **2000**, *23*, 19–26.
- (16) Petro, M.; Svec, F.; Gitsov, I.; Fréchet, J. M. J. *Anal. Chem.* **1996**, *68*, 315–321.
- (17) Muthukumar, M.; Baumgartner, A. *Macromolecules* **1989**, *22*, 1937.
- (18) Hahnfeld, J. L.; Pike, W. C.; Kirkpatrick, D. E.; Bee, T. G. In *Applications of Anionic Polymerization Research*; Quick, R., Ed.; ACS Symp. Ser. **1996**, *696*, 167–184.
- (19) Fernyhough, C. M.; Young, R. N.; Poche, D.; deGroot, A. W.; Bosscher, F. *Macromolecules* **2001**, *34*, 7034–7041.
- (20) Mauran, S.; Rigaud, L.; Coudeville, O. *Transp. Porous Media* **2001**, *43*, 355–376.
- (21) Uhrig, D.; Mays, J. W. *Macromolecules* **2002**, *35*, 7182–7190.
- (22) Meunier, D. M.; Smith, P. B.; Baker, S. A. Patent pending.

MA047862V